Supplementary Information

Surfactant-mediated reduction at water microdroplet interfaces enables switchable synthesis of silver nanoparticles and ammonia

Sinchan Mukhopadhyay, [a] Depanjan Sarkar, *[ab] and Thalappil Pradeep *[abc]

[a] DST Unit of Nanoscience (DST-UNS) & Thematic Unit of Excellence (TUE), Department of Chemistry, Indian Institute of Technology Madras (IITM), Chennai-600036, India.

[b] Centre of Excellence on Molecular Materials and Functions, Department of Chemistry, Indian Institute of Technology Madras,), Chennai-600036, India.

[c] International Centre for Clean Water, 2nd Floor, B-Block, IIT Madras Research Park, Kanagam Road, Taramani, Chennai-600113, India

E-mail: depanjan_coe@icsrpis.iitm.ac.in, pradeep@iitm.ac.in

Table of contents

S1. Experimental section:

Materials

Sodium dodecyl sulfate, , triton X-100, Silver Nitrate, trisodium citrate, salicylic acid, sodium nitroprusside, cetyltrimethylammonium bromide was purchased from Merck Specialities. HPLC grade methanol, n,n-dimethylformamide, dimethyl sulfoxide were purchased from Advent Chembio Pvt. Ltd, India. Sodium hypochlorite AR was purchased from Research-Lab Fine Chem Industries, India. Ultrapure water (resistivity > 18.2 MΩ·cm) was used for all aqueous solution preparations. All the chemicals are commercially available and used as such without any purification.

Reaction setup and experimental details

10 ml of water solution of reactants was taken in a round bottom flask and it was capped tightly with silicone rubber stopper. Then it was purged with Argon by bubbling for 30 mins for deoxygenation purpose. Then the flask was placed in a water bath. In the water bath, a commercial ultrasonic mist maker (1.7 MHz, 24 W) was kept at the bottom externally beneath the flask. Upon turning on the mist maker, microdroplets were generated. When the ultrasonic wave was turned off, microdroplets condensed into bigger droplets and they fell back to the bulk part of the reaction solution.

Characterization

Transmission electron microscopy (TEM) analysis was performed using a ThermoFisher Scientific Talos™ F200i microscope operated at 200 kV. High-angle annular dark-field scanning transmission electron microscopy (HAADF-STEM) imaging, coupled with energy-dispersive X-ray spectroscopy (EDS), was employed to obtain elemental mapping of the particles. Lattice fringes in HRTEM images were measured using ImageJ software. UV vis analysis was performed through LAMBDA® 365 double-beam UV/Vis spectrometer (Perkin Elmer).

Mass spectrometric analysis was performed using an LTQ-XL mass spectrometer (Thermofisher scientific). Nano-electrospray ionization was employed for ionization in the negative mode. Both capillary and tube lens voltages were kept at -5 V to minimize the in-source fragmentation. The data were extracted using Xcalibur software.

Calculation of measuring of particle size distribution from TEM micrograph

The particle size distribution was determined from TEM images using ImageJ software. Briefly, multiple representative TEM micrographs recorded from different regions of the sample were analysed. The image scale was first carefully calibrated using the original scale bar of TEM micrograph. Next, Individual nanoparticles were identified and their diameters measured using the line measurement tool in ImageJ, assuming spherical morphology. Over 250 particles from at least 3 independent micrographs were measured to ensure statistical reliability. The resulting particle diameters were used to construct the size distribution histogram, from which the average particle size was obtained.

Ammonium ion quantification method (modified Berthelot's method[1])

1 M NaOH solution containing 5 wt% salicylic acid and 5 wt% trisodium citrate dihydrate was prepared in Milli-Q water. Two separate solutions of 0.05 M NaClO solution was prepared (from 1 wt% stock solution) in 40 ml and 1 wt% sodium nitroprusside in 10 ml of water. Next, 1 ml of sample were treated with 1.6 mL of 1 M NaOH solution containing 5 wt% salicylic acid and 5 wt% trisodium citrate, followed by 0.40 mL of 0.05 M NaClO solution and 0.12 mL of 1 wt% sodium nitroprusside solution. The mixtures were incubated in the dark at ambient temperature for precisely 2 hours before being transferred into cuvettes for UV-VIS absorption spectroscopy. A calibration curve was generated by plotting the absorbance at 655 nm versus known NH_4^+, and linear regression was performed to determine NH_4^+ concentrations in the samples. To precipitate Ag^+ from the solution, 100 µl of 1M NaCl solution was added to the reaction mixture and the liquid part was analysed for NH_3, after centrifugation. In case of CTAB, after 4 hours of reaction, the reaction mixture was kept in 10 °C, below its Krafft temperature for 2 hours to precipitate CTAB from the solution which was separated by centrifugation. The remaining liquid part was characterized for NH_3.

Optical microscopic images

The droplet samples were collected on glass slides and examined with a Keynes microscope (KEYENCE INDIA PVT. LTD. Model no VHX-950F).

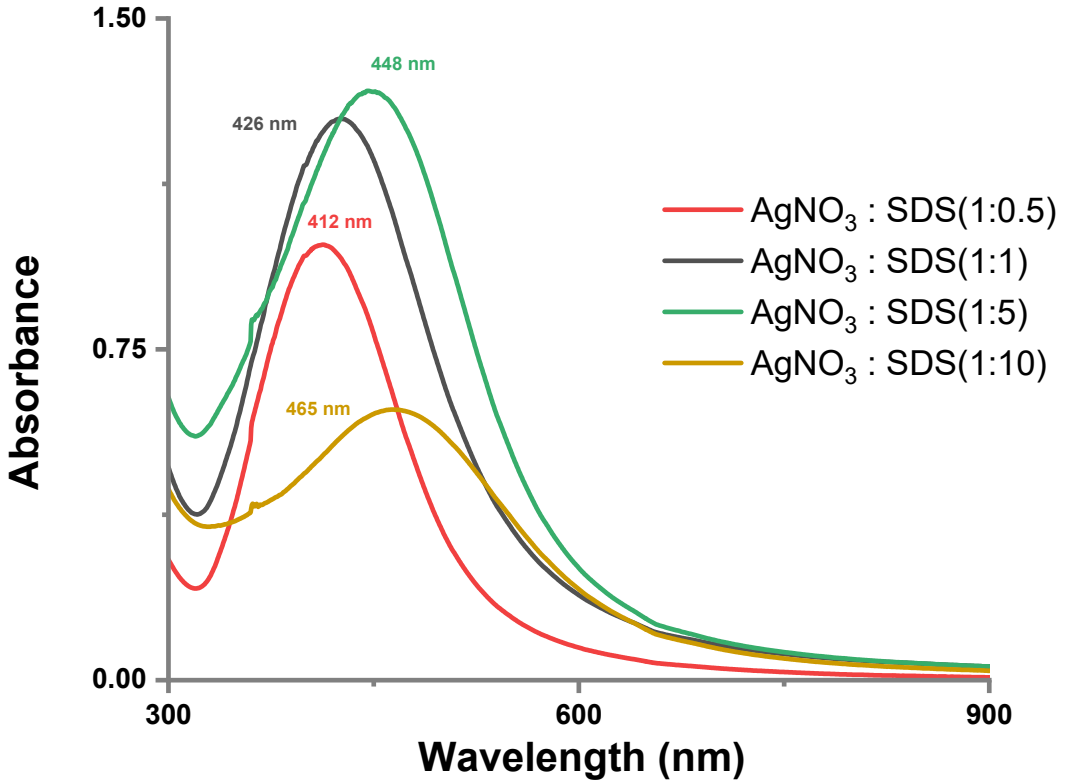

Fig. S1. UV-Vis spectrum of Ag Nanoparticles at different $AgNO_3$: SDS concentration ratio (with respect to $AgNO_3$ = 1 mM).

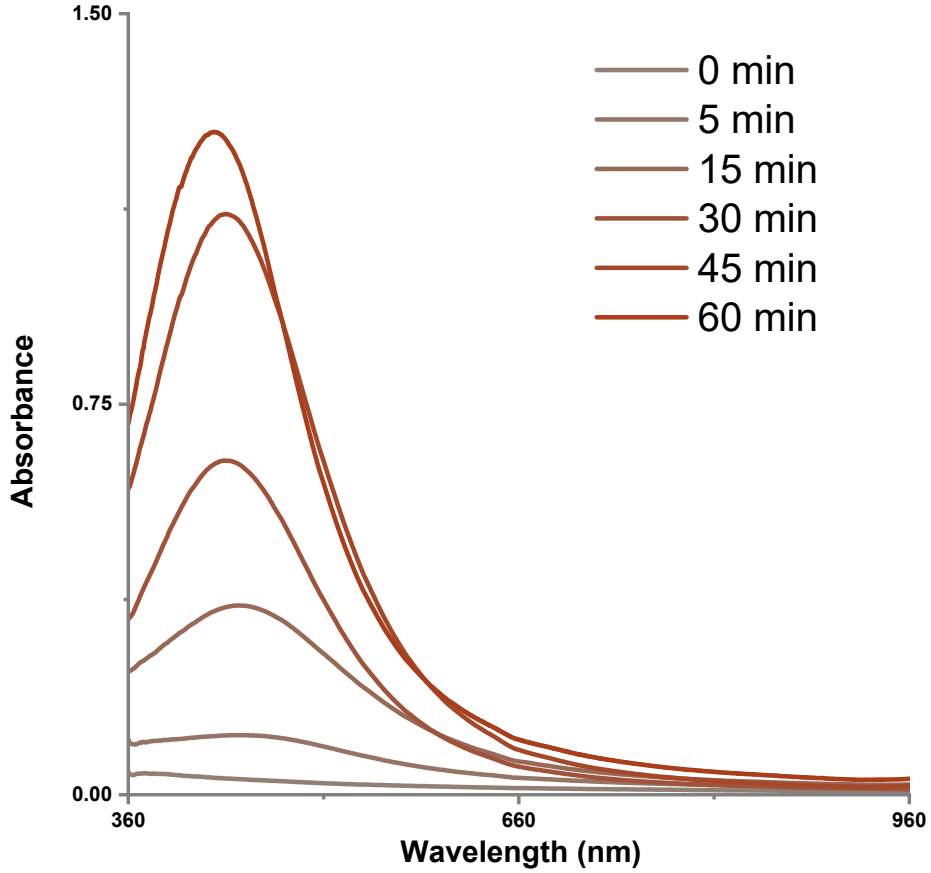

Fig. S2. UV-Vis spectra of the time dependent analysis of Ag NPs**.**

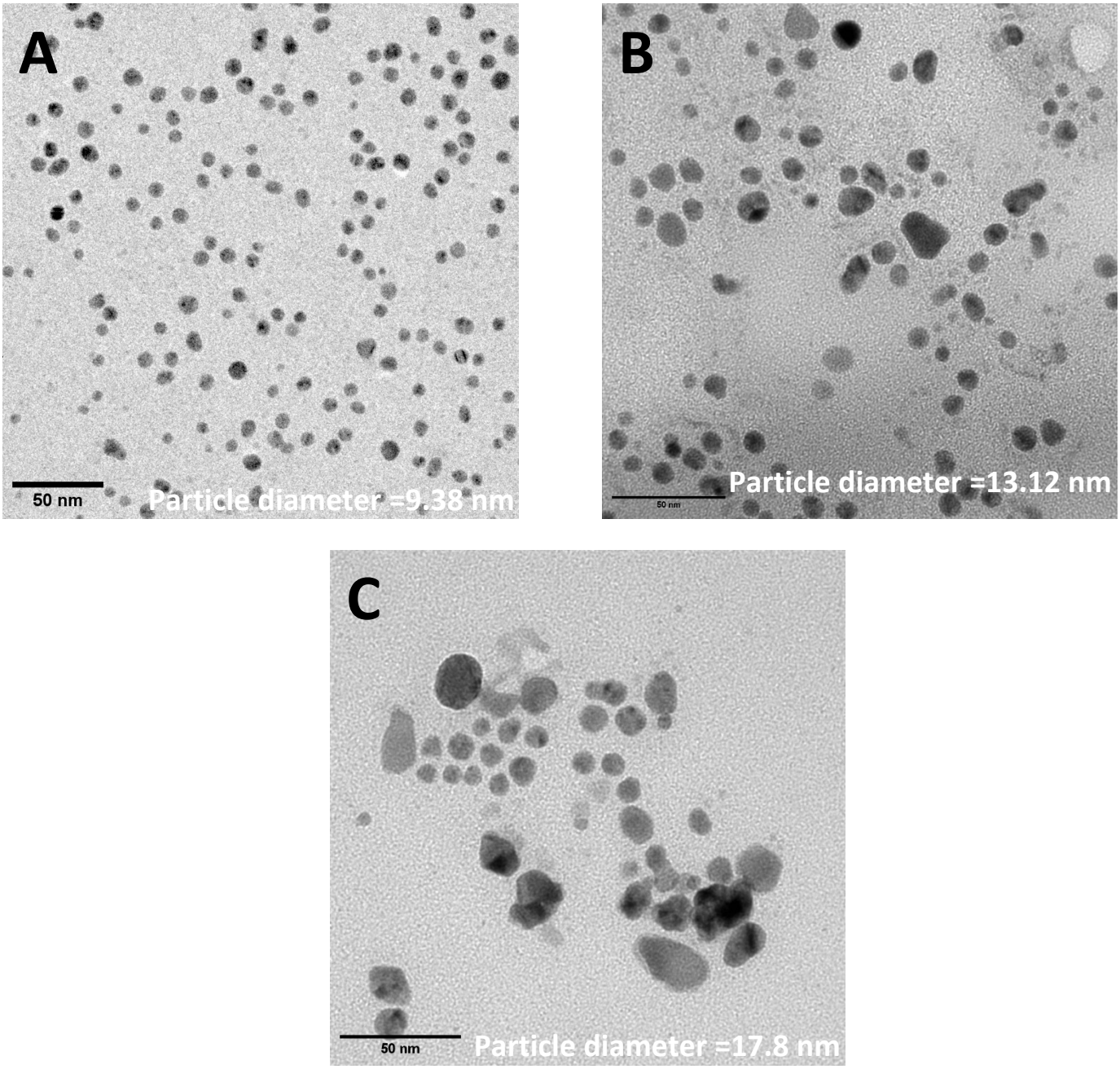

Fig. S3. TEM images of Ag Nanoparticle for $AgNO_3$: SDS at (A)1:0.5, (B) 1: 5 and (C) 1:10.

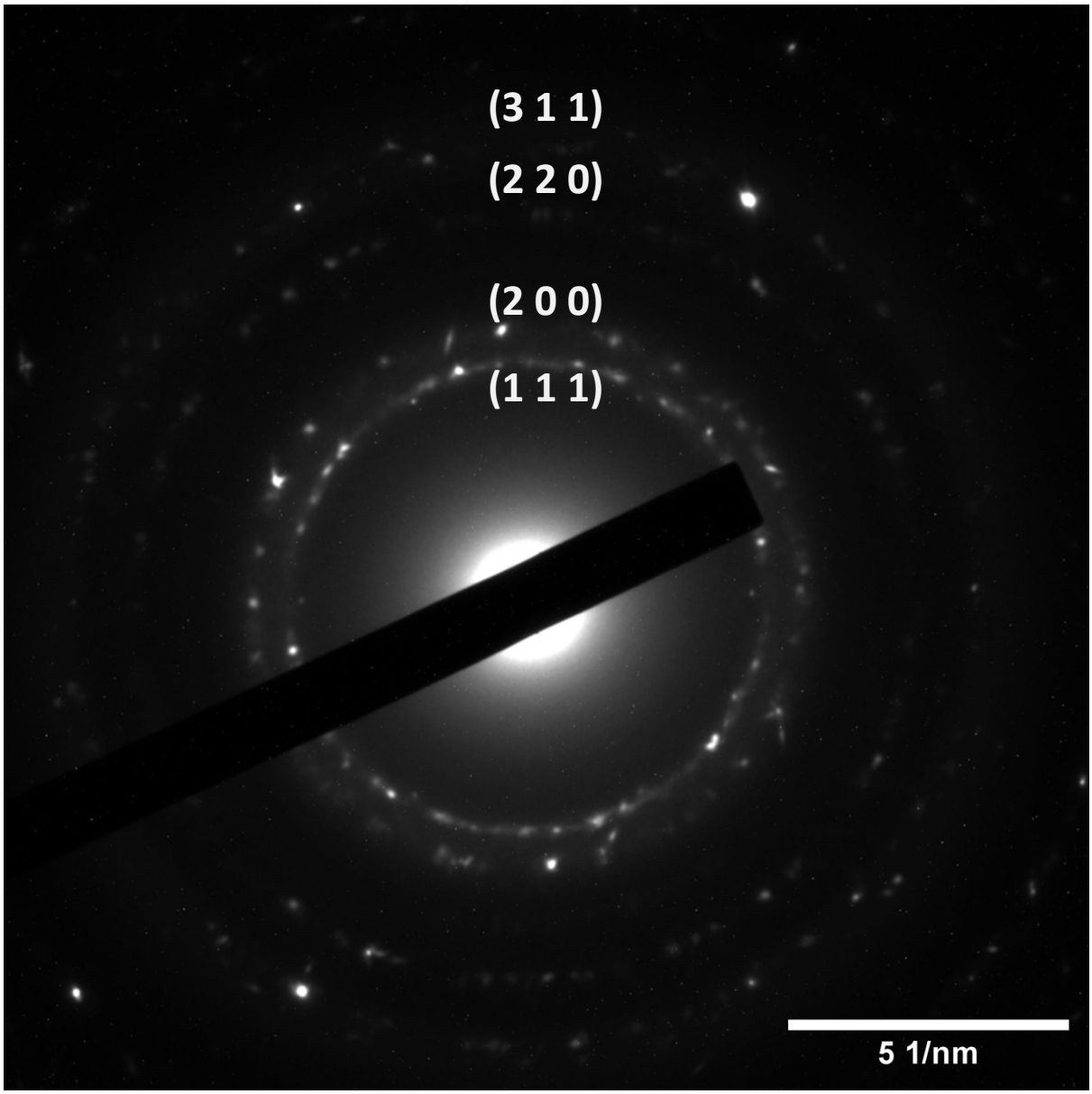

Fig. S4. Selected area electron diffraction (SAED) pattern of Ag NP.

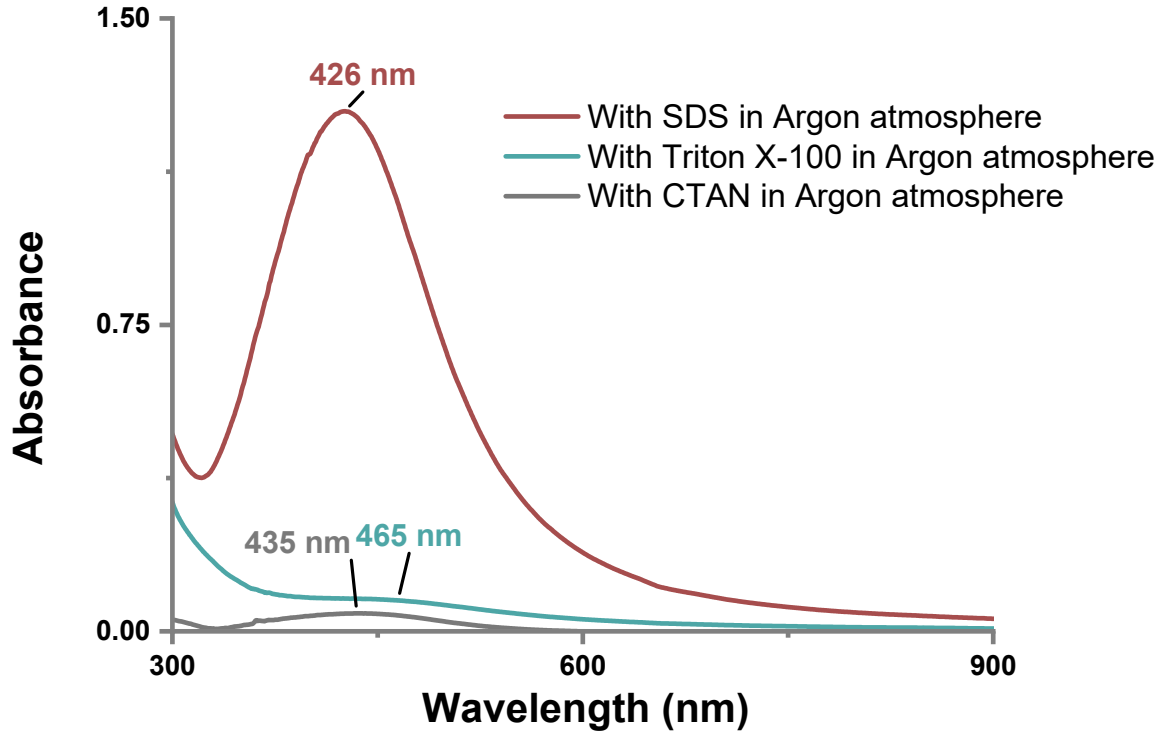

Fig. S5. UV-Vis spectrum of Ag Nanoparticles changing the ionic nature of the surfactants i.e., anionic, cationic and non-ionic.

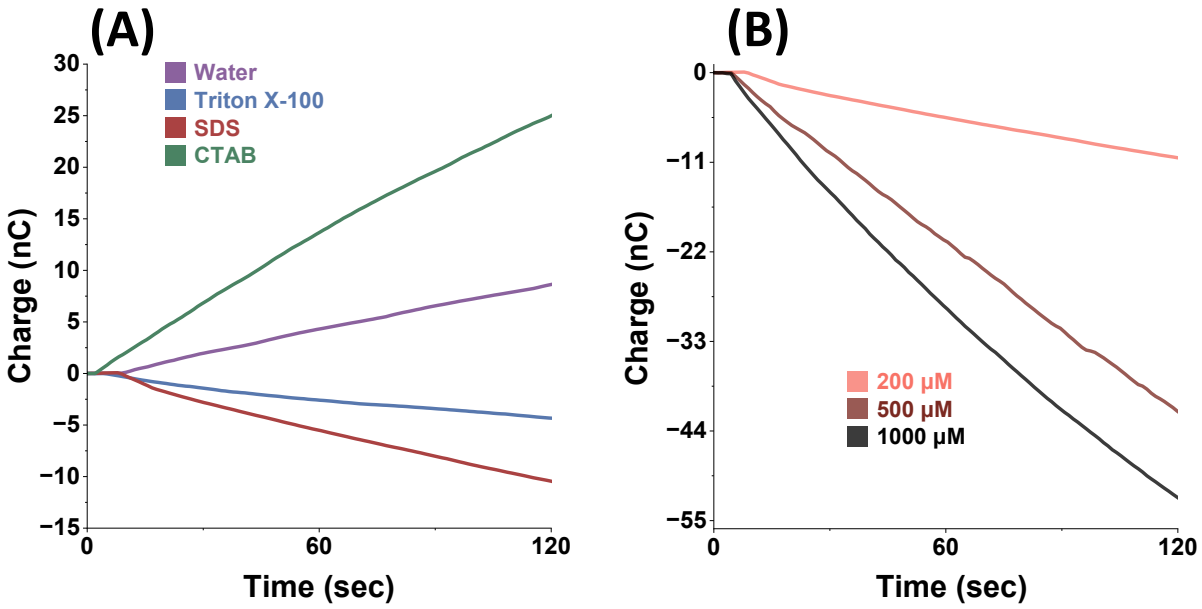

Fig. S6. Measurement of droplet charging using Faraday cup, (A) with different surfactants and (B) upon varying the concentration of SDS. Droplets were continuously deposited in the Faraday cup as a function of time shown in the X-axis.

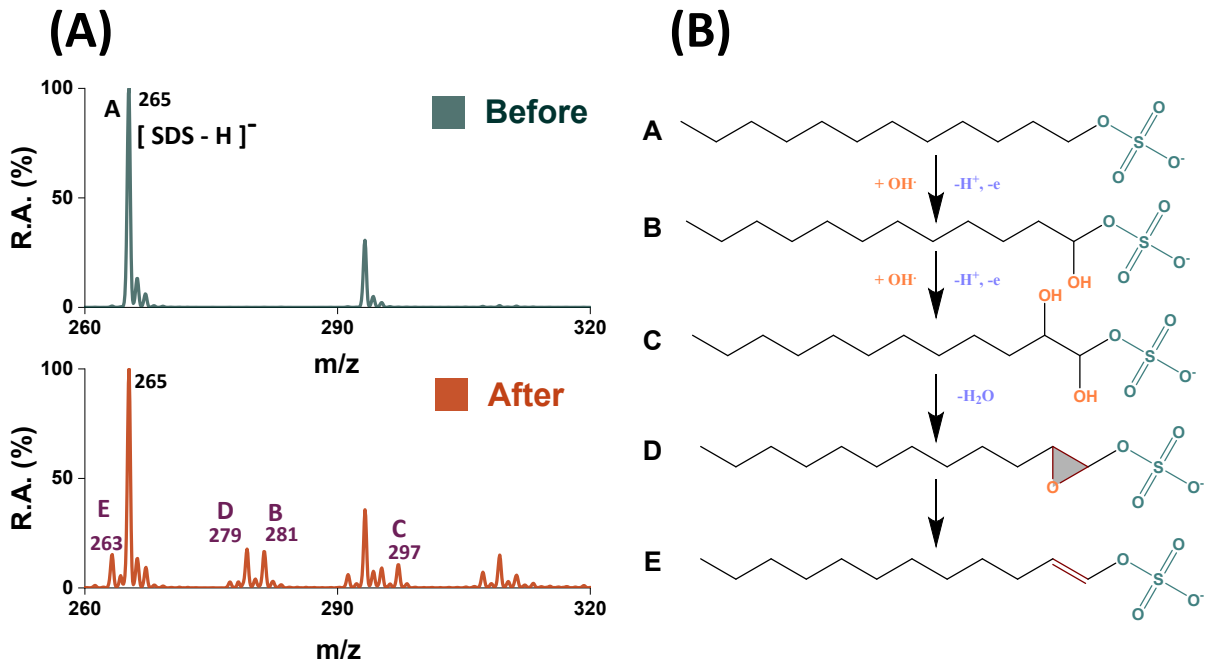

Fig. S7. (A) Mass spectrometric analysis of SDS before and after nebulization and (B) plausible pathway of oxidation of SDS.

Fig. S8. Collison induced dissociation (CID) analysis of SDS and the oxidized species (A) m/z 265, (B) m/z 263, (C) m/z 279, (D) m/z 281 and (E) m/z 297.

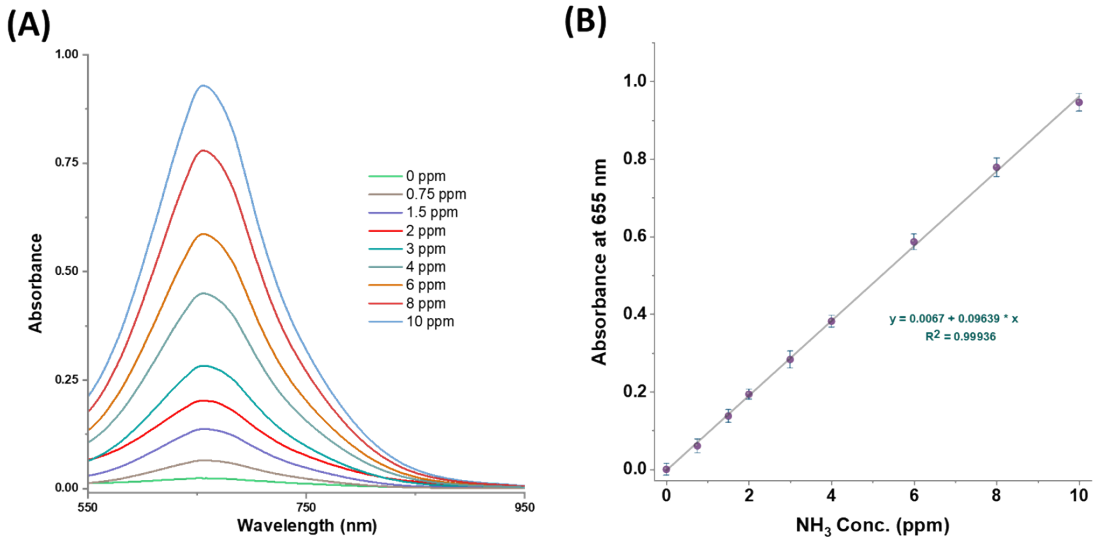

Fig. S9. Quantification of NH_3 using Modified Berthelot's method using series of known concentrations. (A) UV-Vis spectrum and (B) calibration plot using absorbance at 655 nm.

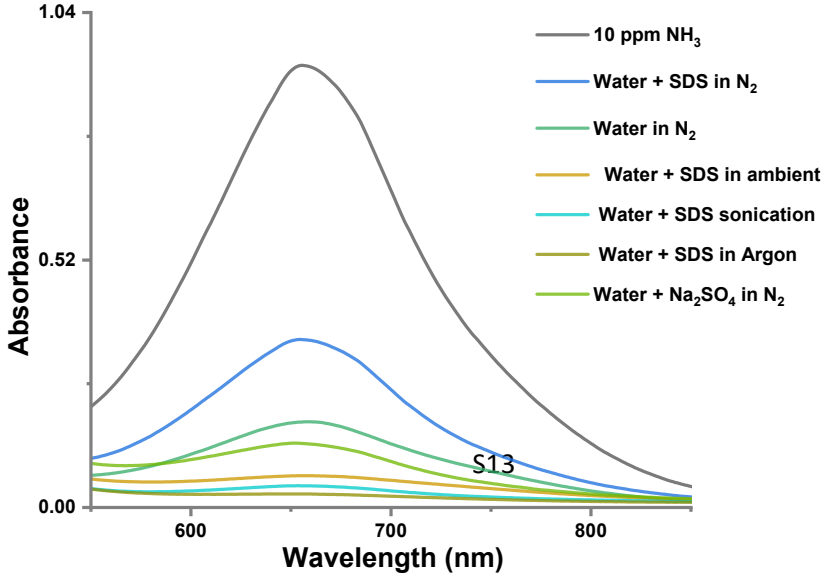

Fig. S10. UV-Vis spectra obtained from Berthelot's method to detect NH_3 at different controlled conditions and the data are compared with standard 10 ppm NH_3.

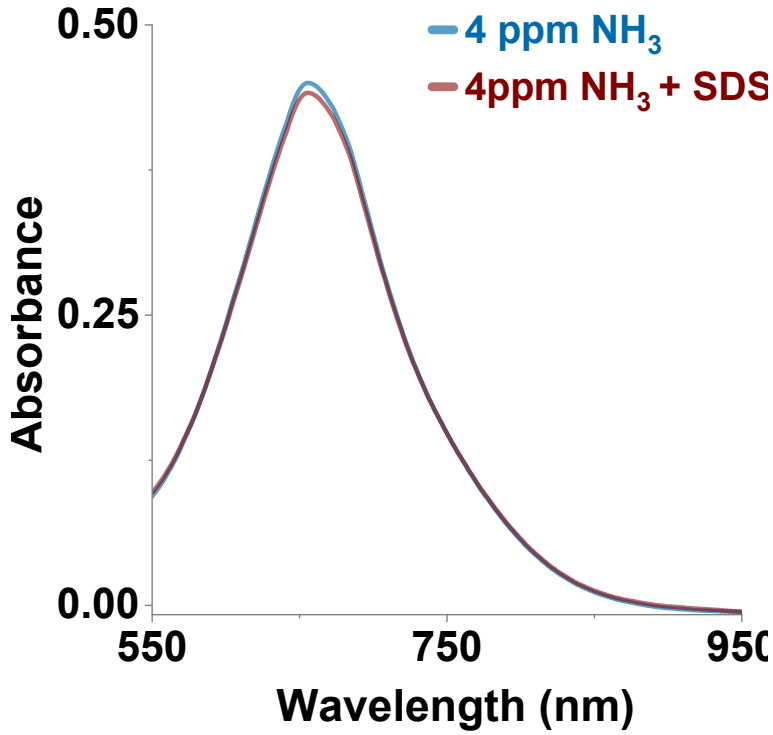

Fig. S11. UV-Vis spectrum of modified Berthelot's method using 4 ppm standard NH_3 with and without SDS.

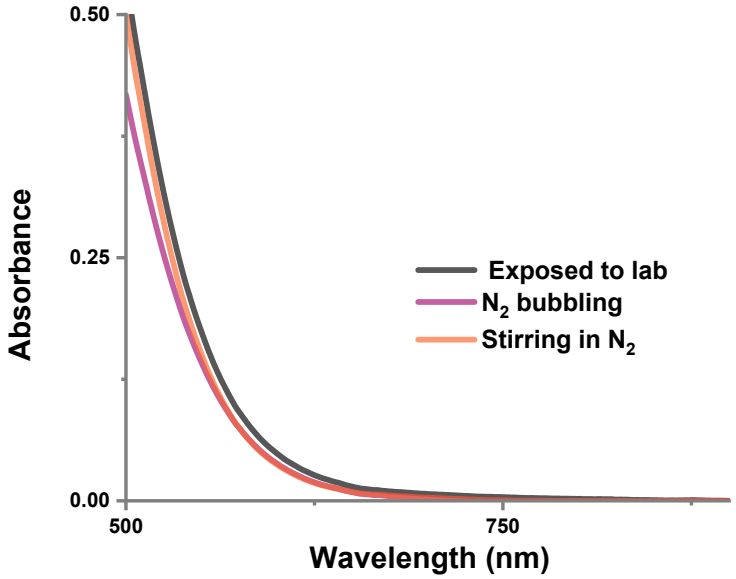

Fig. S12. Control experiments showing no NH_3 formation under atmospheric conditions in the absence of microdroplet production, verifying no contribution from laboratory background nitrogen.

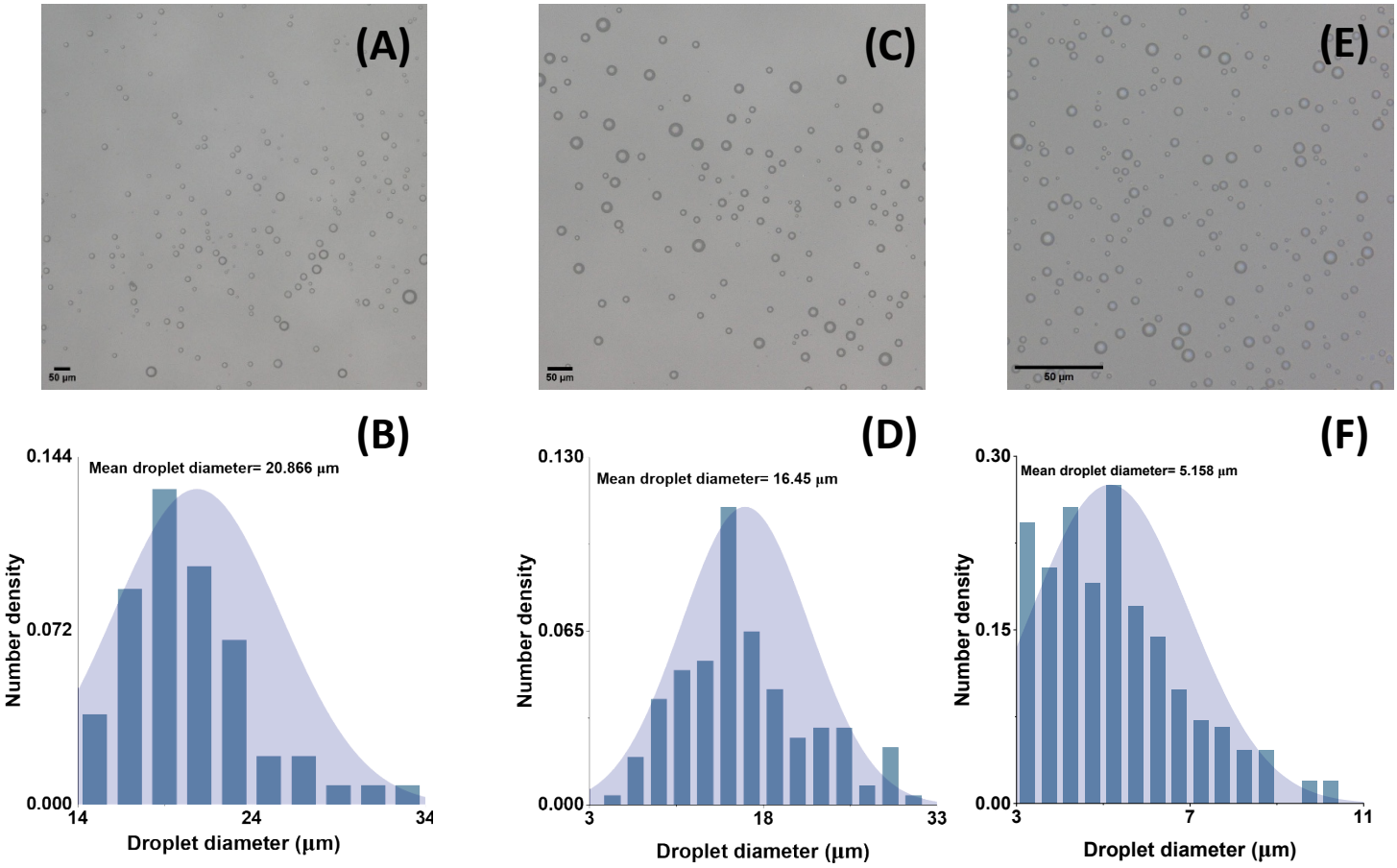

Fig. S13. Optical microscopic images of microdroplets and droplet size distribution for (A) & (B) aqueous solution of Na_2SO_4, (C) & (D) only water and (E) & (F) aqueous solution of SDS.

S2. References:

1. T. M. Vu, S. Johnston, D. Simondson, C. K. Nguyen, T. D. Nguyen, D. V. Zeil, R. K. Hocking, D. R. Macfarlane and A. N. Simonov, *ACS Catal.*, 2024, **14**, 10974–10986.